7. SUPPLEMENTARY INFORMATION

In this section additional information which are supporting the results and conclusions presented in this work are provided.

Note added after first publication: this document replaces the version published on 2nd December 2024, which contained minor errors relating to Figure S5. Specifically, in the caption for Figure S5b, the section '(> 1.9% in this case)' has been corrected to '(< 1.9% in this case)' and in the legend for Figure S5b, 'I_{SC}' has been corrected to 'I_{SC}/GNI'.

7.1 Outdoor Simulation

For the simulation of outdoor spectra using SMARTS2 [26], the following parameter have been varied between the given ranges, while all possible combinations of Airmass, Aerosol Optical Depth and Precipitable Water have been considered.

Parameter	Airmass	Aerosol Optical Depth	Precipitable Water Fine	Precipitable Water Rough
Min.	1	0	0	0.8
Max.	6	0.36	0.9	4
Step	0.1	0.06	0.1	0.2

Table S 1: Parameter variation for the simulation of outdoor spectra using SMARTS2.

For the simulation results presented in Figure 3 the short-circuit current densities of the module $j_{SC_{module}}$ have been determined according to eq. 9 to eq. 11. For the monofacial configuration the rear side contribution to $j_{SC_{bot}}$ in eq. 10 is discarded. For the top-cell configuration only eq. 9 was used.

$$j_{SC_{top}} = \int SR_{top}(\lambda) \cdot E_{sim}(\lambda)\, d\lambda \tag{9}$$

$$j_{SC_{bot}} = \int SR_{bot,front}(\lambda) \cdot E_{sim}(\lambda)\, d\lambda + \int SR_{bot,rear}(\lambda) \cdot E_{rear}(\lambda)\, d\lambda \tag{10}$$

$$j_{SC_{module}} = min(j_{SC_{top}}, j_{SC_{bot}}) \tag{11}$$

In those equations SR_{top}, $SR_{bot,front}$ and $SR_{bot,rear}$ are representing the spectral responsivities of the top- and bottom-cell, E_{sim} and E_{rear} the front and rear side incident spectrum and $j_{SC_{top}}$ and $j_{SC_{bot}}$ the short-circuit current densities of the top- and bottom-cell under the respective spectral conditions.

7.2 Outdoor Measurement Setup and Hysteresis in IV-Curves

To cover the rear side of the module during outdoor measurements an aluminum sheet of 1 mm thickness painted with a spectrally broadband low reflective black coating was used. The temperature of the module was tracked using a Pt100 temperature sensor which was attached to the glass back sheet of the device.

Forward *IV* scans with a sweep time of 10 s have been performed using a four-quadrant power supply unit in combination with different shunt resistors. To estimate the uncertainty introduced by only performing forward *IV* scans, indoor measurements were carried out. These indoor measurements involved performing both forward and reverse scans under different spectral conditions, which resulted in a limitation of the top and bottom-cell respectively. During indoor measurements, the single-cell module was only illuminated from the front. A scan speed of 10 s was chosen to ensure comparability with the outdoor measurement. An LED based solar simulator was used for the indoor measurements,

and the spectral adjustment was performed following the procedure introduced in [34].
To create top-cell limiting conditions, the intensity on the top-cell was reduced by 15%, while the same intensity was added to the bottom-cell, resulting in a Z_{12} value of -0.15 (SMR12g = 0.74). For bottom-cell limiting conditions, a Z_{12} value of 0.03 (SMR12g = 1.03) was chosen. The resulting normalized *IV* curves can be seen in Figure S 1.

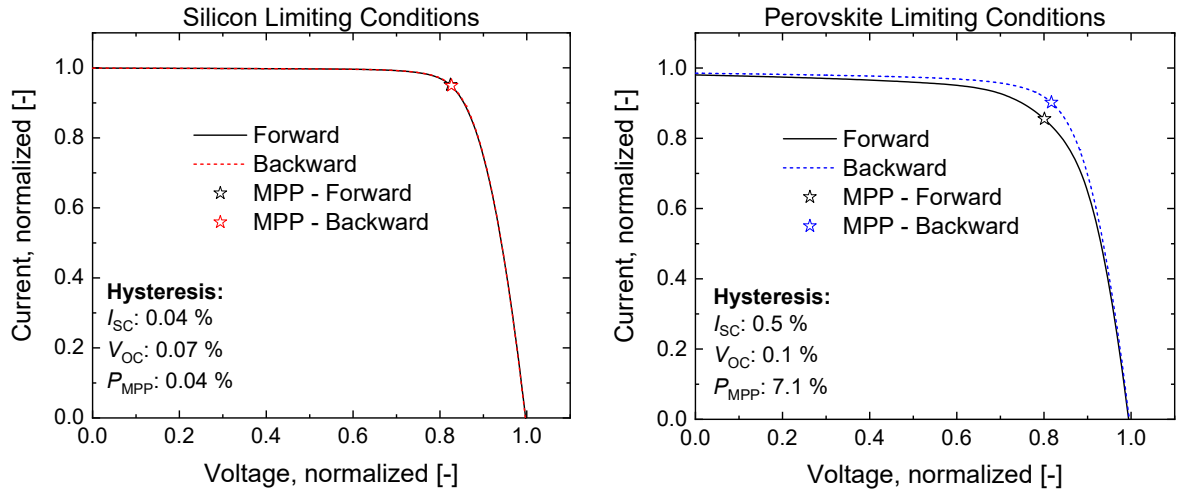

Figure S 1: Forward and Backward IV curves measured under a) bottom and b) top-cell limiting spectral conditions. An LED based solar simulator was used for the measurement carried out with a scan speed of 10 s.

Under bottom-cell limiting conditions, no hysteresis is observed, and therefore, using only the data from the forward *IV* scan is sufficient for evaluating all *IV* parameters. However, under top-cell current limitation, a significant hysteresis is visible for the P_{MPP}. Therefore, considering only the forward *IV* scan underestimates the real P_{MPP} of the device. The primary focus of this work is on the device I_{SC}, where the hysteresis is comparatively small even under top-cell limiting conditions. During AM1.5g spectral conditions the silicon bottom-cell limits the device current, such that the hysteresis does not influence the determination of the modules $\sigma_{I_{SC}}$ and $\sigma_{P_{MPP}}$ presented in section 6. Therefore, the limitation of the measurement setup does not substantially affect the presented results, as can be concluded from Figure S 1 b). However, if the procedure introduced in this work is used for outdoor module calibration performing P_{MPP} tracks to determine the modules $\sigma_{P_{MPP}}$ should be preferred.

7.3 Component Cell Sensor

The EQE of the three component cells used for the assessment of the outdoor spectral conditions throughout this work are plotted together with the AM1.5g reference spectrum [19] in Figure S 2. Outdoor spectral conditions are mainly affected by three parameters which are: “Airmass”, “Aerosol Optical Depth” and “Precipitable Water” [35]. The bandgaps of the component cells have been chosen to investigate the influence of those three main parameters separated to some extend and therefore provide a good measurand for the spectral distribution of the actual outdoor spectrum [29].

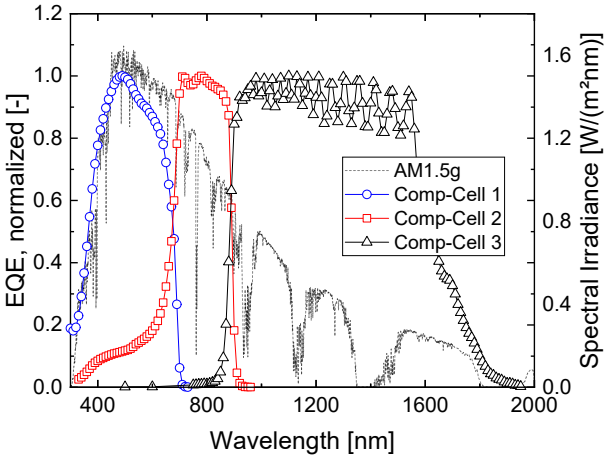

Figure S 2: EQEs of the three component cells used together as component cell sensor to evaluate outdoor spectral conditions. The AM1.5g reference spectrum is plotted as dashed line in the background.

7.4 Filtering Parameters

Measured datapoints are excluded from the evaluation if one (or more) of the following conditions is met:

- DNI/GNI < 0.6
- $I_{MPP}/I_{SC} > 1.0$
- $V_{MPP}/V_{OC} > 1.0$
- Sun pointing error Azimuth (x) > 0.5°
- Sun pointing error Elevation (y) > 0.5°
- SMR12g > 2
- $\left|\left(1 - \frac{GNI_{before\ I-V\ scan}}{GNI_{after\ I-V\ scan}}\right)\right| \cdot 100 > 1.0\ \%$
- RSI > 500 W/m²
- RSI < 0 W/m²
- GNI < 0 W/m²
- Module rear side temperature > 100 °C
- Module rear side temperature < 0 °C

For the investigated dataset 26% of the total data recorded have been excluded based on these conditions.

For the determination of the bifacial yield parameters $^{\sigma_{I_{SC}}}$ and $^{\sigma_{P_{MPP}}}$ datapoints are additionally excluded if one (or more) of the following conditions is met [29].

- GNI min-max variation 10 min before the measurement ≥ 10%
- GNI min-max variation in 30 min ≥ 40%
- GNI < 800 W/m² or GNI > 1200 W/m²
- DNI/GNI < 0.8
- SMR12g < 0.97 or SMR12g > 1.03
- SMR13g < 0.97 or SMR13g > 1.03
- SMR23g < 0.97 or SMR23g > 1.03
- 5 min average wind speed < 0.5 m/s or 5 min average wind speed > 5 m/s

Based on this stricter filter criteria, 83% of the data points were excluded.

7.5 Global Normal and Rear Side Irradiance

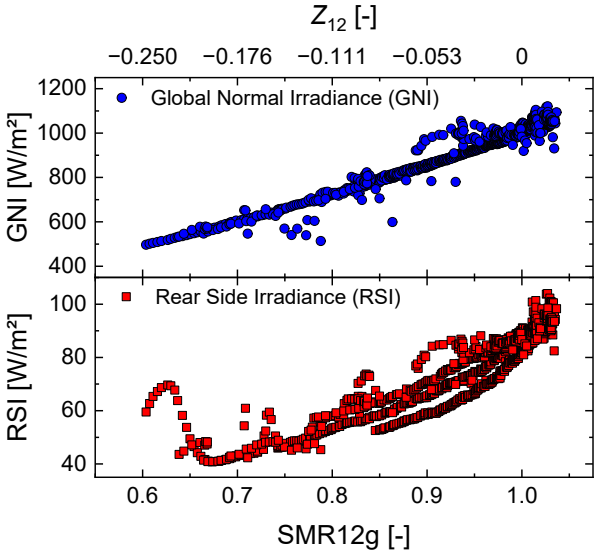

Figure S 3: GNI (top) and RSI (bottom) plotted versus SMR12g. The presented values were measured using a forward and a backward facing pyranometer.

7.6 V_{OC} Evolution

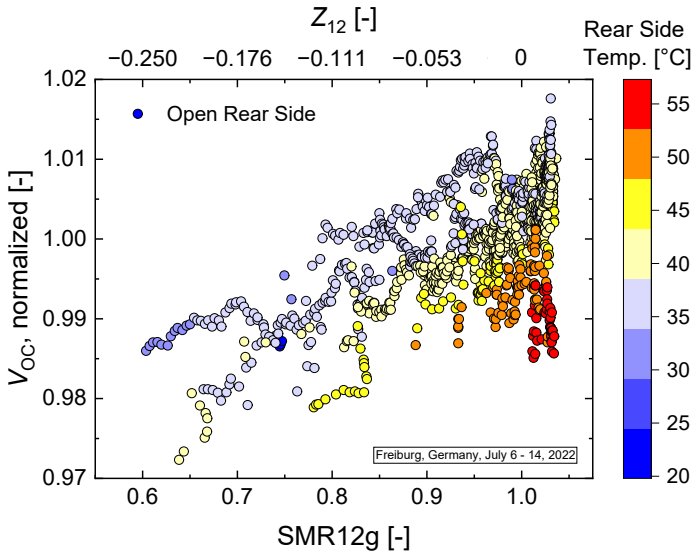

Figure S 4: V_{OC} versus SMR12g measured with an open rear side. The color-code represents the rear-side temperature of the module. The increase in V_{OC} towards higher SMR12g values can be explained by the simultaneous increase in the integral irradiance over the course of a day. The decrease in V_{OC} with increasing temperature is shown by the color-code.

7.7 Determination of Temperature Coefficients

For the determination of temperature coefficients another identically constructed single-cell module, equipped with a thermocouple (Type K) directly attached to the cell's rear side and laminated into the module, was build. Laminating the thermocouple into the module instead of attaching it to the module's rear side enables a more precise determination of the cell's temperature and also prevents the temperature sensor from becoming detached during the measurement.

Using this module, shown in Figure S 5 a), thermal transient measurements (TTMs) [29] have been performed outdoors. During the TTMs the module was mounted on a dual axis tracker as described in section 0. To cool down the module, it was covered with a cardboard. After a temperature difference of at least 20 K compared to the initial temperature measured under illumination was reached the cardboard

was removed and *IV* curves with a sweep time of 10 s have been performed every minute. Due to the incident illumination the module's temperature was rising again. Temperature coefficients are extracted from linear fits applied to the resulting *IV* parameter versus temperature graphs, exemplarily presented for one TTM in Figure S 5 b) to d). The temperature coefficients used for the temperature correction are the mean values determined from three valid TTMs and are provided together with the maximum deviations in Table S 2.

Temperature Coefficient	I_{SC} (α)	V_{OC} (β)	P_{MPP} (γ)
Value [%/K]	0.1 (± 0.02)	-0.16 (+ 0.01)	-0.19 (+ 0.01 – 0.02)

Table S 2: Temperature coefficients determined on a single-cell PSC/Si module equipped with a thermocouple (Type K) attached to the cell's rear side and laminated into the module. The temperature coefficients have been determined in outdoor thermal transient measurements (TTMs).

To consider a TTM as valid the criteria proposed by Steiner et al. [29] which have been adapted for flat plate tandem modules from IEC 62670-3 [36] have been used. The criteria together with the evaluation results for the three TTMs used to determine the temperature coefficients in this publication are provided in Table S 3.

TTM No.	1	2	3
At least 10K difference	x	x	x
At least 5 min. and 10 datapoints	x	x	x
Max. GNI deviation < 0.5% before and after each *IV* sweep	0.6%	x	x
Deviation between max. and min. GNI ≤ 2%	x	x	x
800 W/m² < GNI 1200 W/m²	x	x	x
SMR12g, SMR13g and SMR23g within ±5% of unity	x	x	x
Wind speed below 5 m/s	x	x	x
Ambient temperature change < 1 °C	x	x	x
Temperature coefficient of *FF* within -0.1 and 0%/K	x	-0.11%/K	-0.15%/K
R² of V_{OC} vs. temperature fit > 0.9975	0.9974	x	0.9971

Table S 3: Evaluation criteria and results for the utilized TTM measurements according to [29].

Even though not all criteria have been met for the three TTMs, the deviations are still considered as acceptable. In particular, since the criteria proposed in [29] refer to III-V based tandems, whereas in this publication PSC/Si tandems are investigated. For this reason, the criteria relating to the temperature coefficient of the FF and the linearity of the V_{OC} fit might not be suitable for this material combination. However, a detailed investigation and description of suitable TTM criteria for PSC/Si tandem devices is beyond the scope of this publication.

a) b)

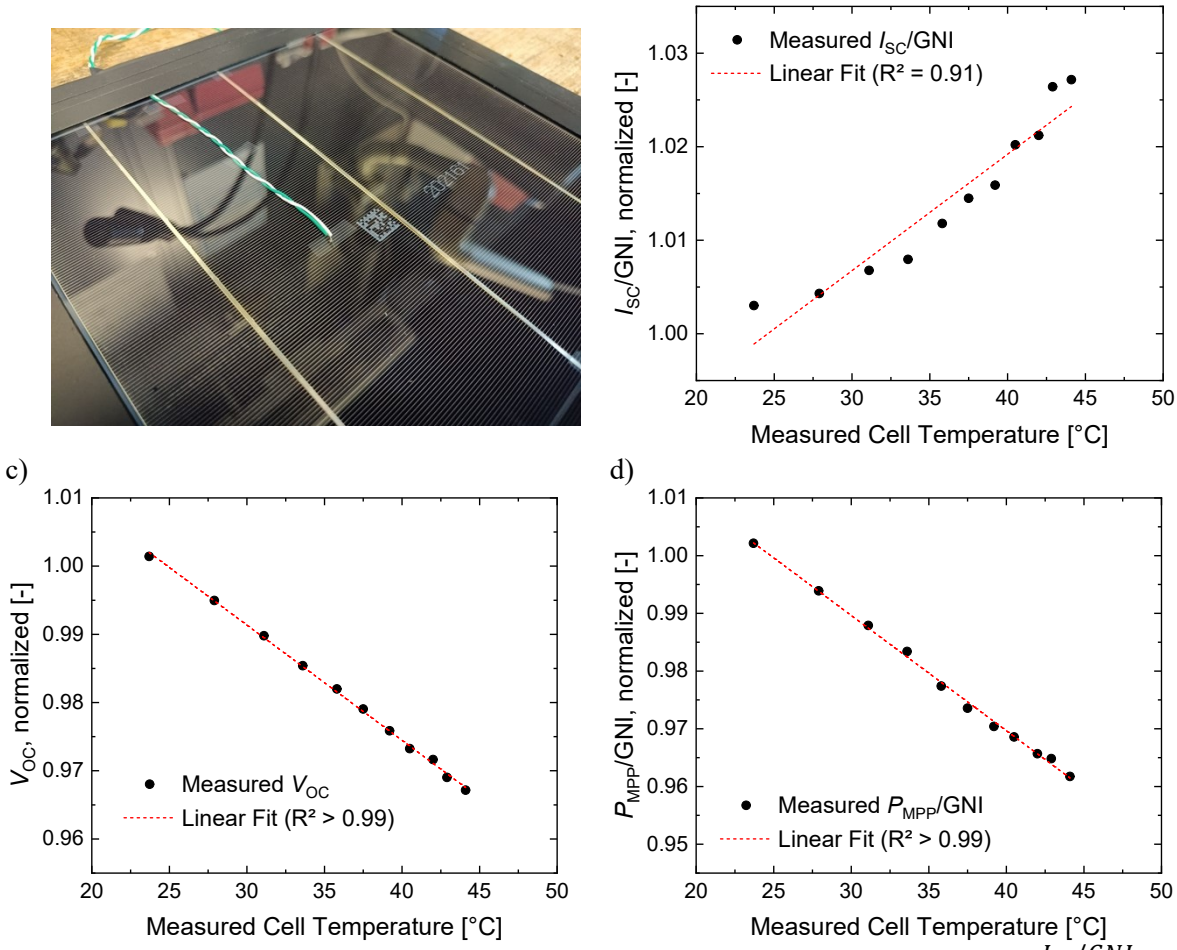

Figure S 5: a) Rear side of the single-cell module used for the determination of temperature coefficients. b) I_{SC}/GNI versus cell temperature. The measured I_{SC} is normalized by the GNI to correct the datapoints for small GNI deviations (<1.9% in this case) throughout the TTM. c) V_{OC} versus temperature. d) P_{MPP}/GNI versus temperature. Just as the I_{SC} also the P_{MPP} is normalized by the incident GNI to correct the influence of GNI deviations within the TTM. All values have been normalized to their respective value determined for a temperature of 25 °C based on the linear fits to the datapoints.

7.8 I_{SC} and P_{MPP} Increase Versus Rear Side Irradiance

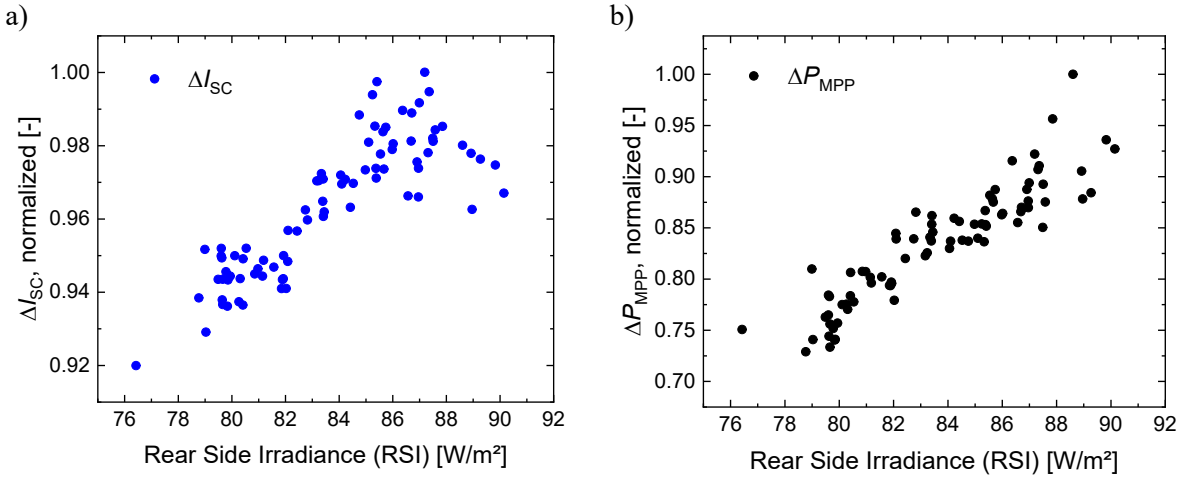

Figure S 6: Evolution of the I_{SC} (left) and P_{MPP} (right) increase plotted versus the incident rear side irradiance (RSI). All data points were normalized to one by dividing them by the respective maximum value. Possible reasons for the deviations from linearity visible in both graphs are uncertainties in module temperature and temperature coefficients as well as in the RSI itself.